# HEAT TRANSFER DURING CONDENSATION OF VAPOR ON A LAMINAR JET OF LIQUID WITH AN INITIAL SEGMENT

N. S. Mochalova, L. P. Kholpanov,
V. A. Malyusov, and N. M. Zhavoronkov

UDC 536.2

Heat transfer during condensation of vapor on a laminar jet of liquid is numerically analyzed, taking into account the initial segment.

Condensation of vapor directly on a cooling heat carrier is promising on account of the high intensity of this process. Such processes occur in mixing preheaters, condensers, and various power-plant components. Only too few and insufficiently thorough theoretical calculations of heat transfer in mixing condenser plants have been made so far, with not too many experimental data available.

When pure vapor condenses at not too low pressures, then the intensity of condensation is determined principally by the heat-transfer processes in the jet and those depend on the flow pattern, on the interphase friction, on the jet geometry, and on the physical properties of the liquid. The condensation rate is highest along the initial jet segment, where the velocity profile as well as the jet surface evolve most noticeably.

This problem was first considered by Kutateladze [1]. With some modifications, it was considered in subsequent studies [2, 3].

The dependence of vapor condensation on a jet on the initial profile has not been theoretically treated, and yet experimental data pertaining to the initial segment [2] seem to differ appreciably from calculations.

It will be assumed that a jet of liquid with an initial temperature $T_0$ discharges through a circular orifice at x = 0, with a radius $R_0$ and a given velocity distribution over its cross section, into a space containing saturated vapor of this liquid at the temperature $T_s$, the radical temperature gradient in the jet being much larger than the axial one. In this case the equations of momentum and energy for laminar flow of such a jet are

$$u\frac{\partial u}{\partial x}+v\frac{\partial u}{\partial y}=-\frac{1}{\rho}\frac{\partial P}{\partial x}+g+\nu\left(\frac{\partial^2 u}{\partial y^2}+\frac{1}{y}\frac{\partial u}{\partial y}\right), \tag{1}$$

$$\frac{\partial (yu)}{\partial x}+\frac{\partial (yv)}{\partial y}=0, \tag{2}$$

$$u\frac{\partial T}{\partial x}+v\frac{\partial T}{\partial y}=a\left(\frac{\partial^2 T}{\partial y^2}+\frac{1}{y}\frac{\partial T}{\partial y}\right). \tag{3}$$

The initial and boundary conditions are

$$\begin{aligned}&\text{at } x=0 \quad u=U_0, \quad T=T_0;\\ &\text{at } y=0 \quad \frac{\partial u}{\partial y}=v=0, \quad \frac{\partial T}{\partial y}=0;\\ &\text{at } y=H(x) \quad \frac{\partial u}{\partial y}=0, \quad T=T_s.\end{aligned} \tag{4}$$

With the aid of the dimensionless variables

Institute of New Problems in Chemistry, Academy of Sciences of the USSR, Moscow. Translated from Inzhenerno-Fizicheskii Zhurnal, Vol. 40, No. 4, pp. 581-585, April, 1981. Original article submitted March 11, 1980.

0022-0841/81/4004-0337$07.50  

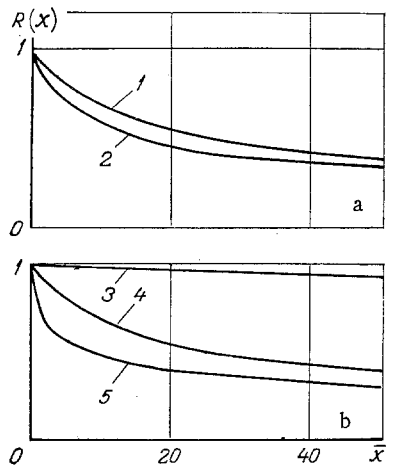


Fig. 1

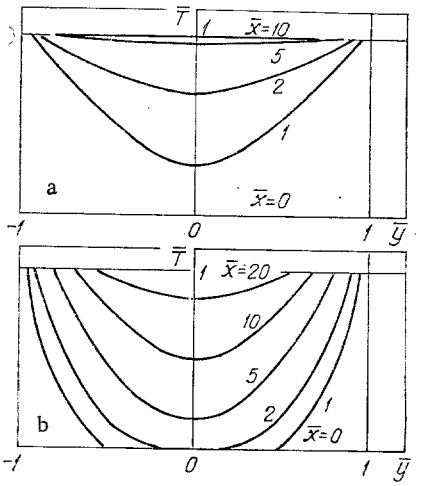


Fig. 2

Fig. 1. Dependence of the dimensionless jet radius on the dimensionless jet length: a) $N_{We}$ = 0.5; 1) $N_{Re}$ = 772; 1000; 2) $N_{Re}$ = 200; b) $N_{Re}$ = 772; 3) $N_{We}$ = 0.001; 4) 0.05; 5) 5.

Fig. 2. Evolution of the dimensionless temperature profile at various distances from the jet discharge orifice ($N_{Re}$ = 772; $N_{We}$ = 0.05): a) $N_{Pr}$ = 7; b) $N_{Pr}$ = 50.

$$x = R_0\bar{x};\quad y = \frac{R_0}{C^{1/4}}\bar{y};\quad u = \frac{\nu C^{1/2}}{R_0}\bar{u};$$

$$v = \frac{\nu C^{1/4}}{R_0}\bar{v};\quad P = \rho\frac{\nu^2 C}{R_0^2}\bar{P};\quad \bar{T} = \frac{T - T_0}{T_s - T_0}, \tag{5}$$

where $C = \frac{gR_0^3}{\nu^2}$, the system of equations (1)-(3) can be reduced to the form

$$u_k\frac{du_k}{dx} = \frac{1}{\mathrm{We}}\frac{1}{H^2(x)}\frac{dH}{dx} + \left(\frac{\partial^2 u_k}{dy_k^2} + \frac{1}{y_k}\frac{\partial u_k}{\partial y_k}\right) + 1, \tag{6}$$

$$\frac{dy_k}{dx} = A_k\frac{B_N}{1 - A_N} + B_k, \tag{7}$$

$$u_k\frac{dT_k}{dx} = \frac{1}{\mathrm{Pr}}\left(\frac{\partial^2 T_k}{\partial y_k^2} + \frac{1}{y_k}\frac{\partial T_k}{\partial y_k}\right), \tag{8}$$

convenient for numerical integration by the method shown earlier [4].

The system of equations (6)-(8) was integrated by the Runge–Kutta method. The numerical solution has yielded the shape of the jet as well as its longitudinal velocity and temperature profiles.

The dependence of the dimensionless jet radius on the dimensionless jet length at various values of the Reynolds number and the Weber number is shown in Fig. 1. The graph here indicates that the trend of this relation between jet radius and jet length is almost independent of the Reynolds number, but depends noticeably on the Weber number: as the latter increases, the radius decreases faster with increasing length.

The evolution of the dimensionless temperature profile over the jet cross section at various distances from the place of discharge is shown in Fig. 2. At x = 0 the initial temperature $T_0$ ($\bar{T}$ = 0) is given. The jet is then heated from its surface, where the temperature is $T_s$ ($\bar{T}$ = 1), the temperature profile bends and then becomes flat again, i.e., the jet has been heated entirely to the temperature $T_s$ ($\bar{T}$ = 1). This process becomes faster at lower values of the Prandtl number, but the shape of the temperature profile depends neither on the Reynolds number nor the Weber number.

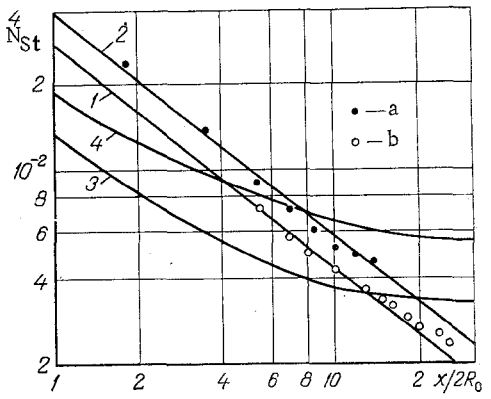


Fig. 3. Dependence of the Stanton number on the dimensionless jet length: (a) $N_{Re}$ = 473; (b) $N_{Re}$ = 772.

In order to determine the local thermal flux density at the jet surface $\lambda(\partial T/\partial y)_{R(x)}$, we multiply Eq, (2) by T and Eq. (3) by y before adding them:

$$\frac{\partial (yuT)}{\partial x} + \frac{\partial (yvT)}{\partial y} = ya\left(\frac{\partial^2 T}{\partial y^2} + \frac{1}{y}\frac{\partial T}{\partial y}\right).$$

Integration of the resulting equation over the jet radius, for a constant flow rate $\int_0^R yudy =$ const, yields the relation

$$aR\left(\frac{\partial T}{\partial y}\right)_R = \frac{d}{dx}\int_0^R yuTdy, \tag{9}$$

from which we obtain the expression

$$\lambda\left(\frac{\partial T}{\partial y}\right)_R = \frac{\rho C_p}{R}\frac{d}{dx}\int_0^R yuTdy \tag{10}$$

for the local thermal flux density. The mean heat-transfer coefficient from the jet surface is

$$\alpha = \frac{1}{\Pi\Delta T}\int_0^x 2\pi R(x)\,\lambda\left(\frac{\partial T}{\partial y}\right)_R dx, \tag{11}$$

where $\Pi$ denotes the area of the contact surface between liquid and vapor

$$\Pi = \int_0^x 2\pi R(x)\,dx. \tag{12}$$

With relation (10), the expression for the mean heat-transfer coefficient becomes

$$\alpha = \frac{\rho C_p}{\Pi\Delta T}\int_0^x 2\pi\frac{d}{dx}\int_0^R yuTdydx \tag{13}$$

or in terms of dimensionless variables

$$\alpha = \frac{C^{1/4}\rho C_p \nu \int_0^{\bar{R}} \bar{y}\bar{u}Td\bar{y}\Big|_0^{\bar{x}}}{R_0\int_0^{\bar{x}}\bar{R}(x)\,d\bar{x}}. \tag{14}$$

We now introduce the dimensionless Stanton number

$$N_{St} = \frac{\alpha}{\rho C_p U_0}. \tag{15}$$

Inserting here the expression for the mean heat-transfer coefficient yields

$$N_{St} = \frac{C^{1/4}}{N_{Re}} \frac{\int_0^{\bar{R}} \bar{y}\,\bar{u}T\,d\bar{y}\Big|_0^{\bar{x}}}{\int_0^{\bar{x}} \bar{R}(x)\,d\bar{x}}. \tag{16}$$

A numerical solution of Eqs. (6)-(8), with the Weber number varied from 0.001 to 5, the Reynolds number varied from 200 to 1000, and the Prandtl number varied from 1 to 50, has yielded an approximate (within 5%) expression for the Stanton number

$$N_{St} = f_1 f_2 f_3 \left(\frac{x}{2R_0}\right)^{-0.8}, \tag{17}$$

where

$$f_1 = 1.25\cdot 10^{-2} - 7.5\cdot 10^{-6} N_{Re};\ f_2 = 1.05 - N_{Pr}\left(8\cdot 10^{-3} - 3\cdot 10^{-4}\frac{x}{2R_0}\right);$$

$$f_3 = 1.05 - N_{We}\left(0.4 + 0.1\frac{x}{2R_0}\right) \text{ for } N_{We} \geqslant 0.05;$$

$$f_3 = 1.05 - N_{We} + \frac{x}{2R_0}(0.03 - 0.6 N_{We}) \text{ for } N_{We} < 0.05.$$

It is interesting to compare the proposed theoretical expressions with the experimental data [2] pertaining to the heat released during condensation of water vapor on a laminar water jet. The dependence of the Stanton number on the dimensionless jet length is shown in Fig. 3. Here curves 1 and 2 are based on expression (17) with $N_{We} = 0.05$, $N_{Re} = 772$ and 473, respectively, curves 3 and 4 are theoretical curves based on earlier studies [1, 2] with $1/N_{Re}N_{Pr} = 1\cdot 10^{-4}$ and $2\cdot 10^{-4}$, respectively, and the dots represent experimental data [2, 3].

The graph in Fig. 3 indicates a satisfactory agreement between theoretical and experimental results. The maximum deviation of theoretical values from experimental data does not exceed 10%.

## NOTATION

x, y, coordinates of an orthogonal system tied to the axis of symmetry of the jet; u, v, components of the velocity vector along coordinates x, y, respectively; T, temperature; $\nu$, kinematic viscosity; $a$, thermal diffusivity; $\rho$, density; $\gamma$, coefficient of surface tension; $\lambda$, thermal conductivity; $N_{Re} = U_0 R_0/\nu$, Reynolds number; $N_{Pr} = \nu/a$, Prandtl number; and $N_{We} = \rho\nu^2 C^{3/4}/\gamma R_0$, Weber number.

## LITERATURE CITED


1. S. S. Kutateladze, Basic Theory of Heat Transfer [in Russian], Nauka, Sib. Otd. Akad. Nauk SSSR, Novosibirsk (1970).
2. V. P. Isachenko, Heat Transfer during Condensation [in Russian], Énergiya, Moscow (1977).
3. V. P. Isachenko, S. A. Sotskov, and E. V. Yakusheva, "Heat transfer during condensation of water vapor on a laminar cylindrical water jet," Teploenergetika, No. 8, 72-74 (1976).
4. L. P. Kholpanov, V. Ya. Shkadov, V. A. Malyusov, and N. M. Zhavoronkov, "Analysis of hydrodynamics and mass transfer with an initial segment," Teor. Osn. Khim. Tekhnol., 10, No. 5, 659-669 (1976).